

NASA-TM-87151

NASA Technical Memorandum 87151

NASA-TM-87151 19860004208

Heat Transfer and Pressure Drop Performance of a Finned-Tube Heat Exchanger Proposed for Use in the NASA Lewis Altitude Wind Tunnel

G. James Van Fossen
Lewis Research Center
Cleveland, Ohio

November 1985

LIBRARY 87151

DEC 6 1985

LANGLEY RESEARCH CENTER
LIBRARY, NASA
HAMPTON, VIRGINIA

NASA



NF01477

3 1176 01311 4047

HEAT TRANSFER AND PRESSURE DROP PERFORMANCE OF A FINNED-TUBE
HEAT EXCHANGER PROPOSED FOR USE IN THE
NASA LEWIS ALTITUDE WIND TUNNEL

G. James Van Fossen
National Aeronautics and Space Administration
Lewis Research Center
Cleveland, Ohio 44135

SUMMARY

A segment of the heat exchanger proposed for use in the NASA Lewis Altitude Wind Tunnel (AWT) facility has been tested under dry and icing conditions. The heat exchanger has the largest pressure drop of any component in the AWT loop. It is therefore critical that its performance be known at all conditions before the final design of the AWT is complete.

The heat exchanger segment was tested in the NASA Lewis Icing Research Tunnel (IRT) in order to provide an icing cloud environment similar to what will be encountered in the AWT.

Dry heat transfer and pressure drop data were obtained and compared to correlations available in the literature. The effects of icing sprays on heat transfer and pressure drop were also investigated.

INTRODUCTION

A schematic of the NASA Lewis Altitude Wind Tunnel (AWT) and proposed modifications is shown in figure 1. The heat exchanger must remove the heat added to the air stream by the fan and other systems necessary to conduct tests of engines, inlets, props, and airframes at altitude and in icing conditions. A preliminary engineering report (PER) has been written by the Sverdrup Corporation under contract NAS3-24024-AE. A heat exchanger configuration has been recommended by the contractor.

The heat exchanger has the largest pressure drop of any component in the AWT loop. It is therefore critical that the performance of the heat exchanger be known at all operating conditions before the final design of AWT is complete.

The purpose of this report is to present results of heat transfer and pressure drop tests conducted in the NASA Lewis Icing Research Tunnel on a segment of the recommended heat exchanger. The effects of icing sprays on heat exchanger performance were also investigated.

SYMBOLS

A_f heat exchanger frontal area (cross-sectional area of duct upstream of heat exchanger)

1086-13677 #

E-2623

A_{fin}	total fin heat transfer area
A_{hx}/A_{ts}	ratio of duct cross-sectional area upstream of heat exchanger to tunnel test section cross-sectional area
A_m	minimum free flow area in heat exchanger
A_o	total air side heat transfer surface area
A_R	refrigerant side heat transfer area
d	diameter of heat exchanger tube
F	least squares function defined by equation (12)
h_a	air side heat transfer coefficient
h_R	refrigerant side heat transfer coefficient
k_{air}	thermal conductivity of air
LMTD	log mean temperature difference defined by equation (5)
LWC	liquid water content
\dot{m}	mass flow rate in heat exchanger duct
Pr	Prandtl number of air
P_s	average static pressure
P_{t1}	total pressure at rake tube 1
Q	heat exchanger total heat load defined by equation (4)
q	dynamic pressure upstream of heat exchanger defined by equation (9)
R	gas constant for air
Re	Reynolds number based on heat exchanger tube diameter defined by equation (6)
r_h	hydraulic radius of heat exchanger air side
T_{blk}	bulk temperature of air upstream or downstream of heat exchanger
T_i	temperature nearest rake total pressure tube 1
T_R	refrigerant temperature
U	overall heat transfer coefficient defined by equation (7)
X	fraction of LWC removed upstream of the heat exchanger by turning vanes, fan, etc.

V_1 velocity calculated for rake total pressure tube 1
 Δp pressure drop across heat exchanger
 η air side surface efficiency defined by equation (14)
 η_{fin} fin efficiency
 μ viscosity
 ρ_1 density at rake total pressure tube 1

Subscripts

AWT refers to the Altitude Wind Tunnel
 IRT refers to Icing Research Tunnel
 SEG refers to heat exchanger segment tested in Icing Research Tunnel
 1 refers to conditions upstream of the heat exchanger
 2 refers to conditions downstream of heat exchanger

AWT REQUIREMENTS

Heat Transfer

AWT heat exchanger requirements were taken from the 50 percent PER-section 9 process systems (ref. 1). Heat loads include the fan, steam heated turning vanes, and the heat load due to ice formation. Table I shows the heat loads, flow rates, air temperatures, Reynolds numbers, and the required heat exchanger area-overall heat transfer coefficient product. The area-overall heat transfer coefficient product was calculated assuming a 225 K (-55 °F) constant temperature flooded coil heat exchanger. Reynolds number was calculated based on free stream conditions and a 2.54 cm (1.0 in) diameter tube.

The maximum required overall heat transfer coefficient occurs at the 0.7 Mach number, 10 058 m (33 000 ft) altitude, 244 K (-20 °F) condition. The greatest heat load does not occur at this condition, but the combination of heat load and temperatures required make this the most demanding point for heat exchanger heat transfer performance.

Pressure Drop

The maximum heat exchanger pressure drop occurs at the point of maximum flow rate which is the 0.52 Mach number, 1524 m (5000 ft), 293 K (68 °F) condition.

Icing

The test section icing environment goals for the AWT are:

Static temperature, K (°F)	233 to 273 (-40 to +32)
Liquid water content, gm/m ³	0.1 to 3.0
Volume mean droplet size, μm	5 to 50

Figure 2 shows the present FAA FAR 25 icing envelope along with the AWT goal.

APPARATUS

Icing Research Tunnel

The heat exchanger segment was tested in the NASA Lewis Icing Research Tunnel (IRT). This facility was chosen because it could provide the necessary cold temperatures and icing sprays. A circuit diagram of the IRT with the location of the heat exchanger segment tested is shown in figure 3. This location was chosen because water sprayed from the nozzles upstream of the contraction, must travel through the test section, two sets of turning vanes, and the main drive fan before entering the heat exchanger just as it will do in the proposed AWT configuration.

Refrigeration System

The heat exchanger segment was connected in parallel with the IRT refrigeration system as shown in figure 4. Type E thermocouples and strain gauge pressure transducers were installed in the inlet and outlet refrigerant lines. Refrigerant 12 is used in the IRT system. The inlet line was a 2 in copper tube and the control valve had a C_v of 12. The proposed AWT refrigeration system will have a 4:1 overfeed; refrigerant will exit the heat exchanger as a mixture of three parts saturated liquid and one part vapor. The refrigerant exited the heat exchanger segment tested in IRT with several degrees of superheat indicating that this valve trim was too small. It was thought that this did not seriously affect the overall heat transfer and pressure drop data.

Heat Exchanger

The heat exchanger segment tested was a refrigerant 12 - air heat exchanger constructed of 2.601 cm (1.024 in) outside diameter copper tubes (0.124 cm (0.049 in) wall thickness) with seven helically wound fins per inch. The fins were 0.041 cm (0.016 in) thick and 1.52 cm (0.60 in) high. The heat exchanger segment was 91.44 cm (36 in) wide by 89.92 cm (35.4 in) high. The tubes were arranged in a triangular array 6 rows deep with 15 tubes per row. Spacing between the tubes in each row was 5.748 cm (2.263 in). The heat exchanger segment parameters are given in table I.

Three type E thermocouples were attached to the inlet side of the 2nd, 7th, and 13th "U"-tubes (up from the bottom) that connect the 1st and 2nd rows

of heat exchanger tubes. Three similar thermocouples were attached to the outlet side of the 3rd, 8th, and 14th tubes of the last tube row. The thermocouples were held to the outside of the tubes with hose clamps.

Heat Exchanger Duct

The heat exchanger was installed in the 91.44 x 89.92 cm (36 x 35.4 in) plywood duct shown in figure 5. The duct extended 105.4 cm (41.5 in) upstream and downstream of the heat exchanger segment. The inlet of the duct was rounded with a circular contour of 15.88 cm (6.25 in) radius. Air was pulled past the heat exchanger segment by a centrifugal fan which had axial flow inlet and outlet. The fan had a set of damper vanes at the inlet so the flow could be adjusted from zero to the maximum of about 15.4 kg/sec (34 lbm/sec). The test duct is shown schematically in figure 6.

When the system was first checked out an acoustic resonance was found to exist with the fan damper set at about the 50 percent position. This was partially eliminated by installing a plywood splitter in the duct downstream of the heat exchanger. The splitter was horizontal and divided the duct in half.

The mass flow rate of air in the duct was measured with total pressure rakes constructed as shown in figure 7. Each rake contained 16 total pressure tubes and 8 type E thermocouples. The position of the total pressure and thermocouples tubes corresponded to the centers of equal areas for the rectangular duct. There were two identical rakes upstream and two rakes downstream of the heat exchanger. On the upstream side of the heat exchanger the rakes were installed so they bisected the duct in the horizontal and vertical directions. Downstream of the heat exchanger the vertical rake bisected the duct but the horizontal rake was mounted at a point 3/4 of the duct height up from the bottom. This was necessary due to the splitter downstream of the heat exchanger. When not taking data, the rake total pressure tubes were disconnected from the pressure measuring system and purged with dry air to keep out water and ice. This was accomplished with a shuttle valve; there were not enough of these valves available to purge the static taps in a similar manner.

Thermocouples were all type E and were referenced to a 339 K (150 °F) oven.

Static pressures were measured at both the upstream and downstream rake stations. Eight static taps were located at each station. The static taps were located ± 15.2 cm (6 in) on either side of where the rake penetrated the duct wall.

Both static and total pressures were measured using an electronically scanned pressure (ESP) system. Each pressure was measured by a separate ± 0.007 MPa (1.0 psid) transducer which was read and digitized once every several seconds by a minicomputer. Every 350 scans (about every 10 min) the transducers were automatically calibrated by mechanically connecting them to three separate reference pressures. This was accomplished automatically with a shuttle valve. The three reference pressures were atmospheric pressure and about 0.003 MPa (0.5 psi) above and below atmospheric pressure. The reference pressures were measured with precision digital quartz transducers.

All data were recorded on the laboratory data acquisition system which is described in reference 2. For each data point, 20 "scans" or individual readings of each data channel were recorded. These 20 scans were then averaged to give a single reading for each channel. This helped to eliminate some of the noise present in the system. Because of the electronic multiplexing of the individual data channels to the analog to digital converter, there is a certain offset between data channels. In an extreme case this caused a 0.6 °C indicated difference in thermocouples that were at the same temperature. This was corrected by shorting all the inputs to the data acquisition system after a run, recording this value, then subtracting this "zero" from each reading.

Data Reduction

Duct mass flow rate. - The velocity for each total pressure tube was calculated from the pitot tube equation:

$$V_i = \sqrt{\frac{2(P_{t1} - P_s)}{\rho_i}} \quad (1)$$

where P_{t1} was the total pressure from rake tube i , P_s was the average of the eight static pressure taps, and ρ_i the density calculated from the perfect gas law using the static pressure and the rake temperature nearest total pressure tube i . For example, referring to figure 6, the temperature from thermocouple 5 would be assigned to total pressure tubes 9 and 10. Moisture in the air due to water sprays was neglected in the calculations. The total mass flow rate at each rake was then calculated from

$$\dot{m} = \frac{A_f}{32} \sum_{i=1}^{32} \rho_i V_i \quad (2)$$

where A_f is the cross-sectional area of the duct (0.822 m² (8.85 ft²)).

Bulk temperature. - The upstream and downstream bulk (or mass averaged) temperatures were computed from

$$T_{blk} = \frac{A_f}{32 \dot{m}} \sum_{i=1}^{32} \rho_i V_i T_i \quad (3)$$

where T_i is the temperature nearest total pressure tube i .

Heat load. - The heat exchanger heat load was calculated from

$$Q = \dot{m}_1 C_p (T_{blk1} - T_{blk2}) \quad (4)$$

where \dot{m}_1 is the mass flow rate from the upstream rakes, C_p is the specific heat of air, T_{blk1} is the upstream bulk temperature and T_{blk2} is the downstream bulk temperature.

Log mean temperature difference (LMTD). - The LMTD was calculated from

$$\text{LMTD} = \frac{(T_{b1k1} - T_{R1}) - (T_{b1k2} - T_{R2})}{\ln \left(\frac{T_{b1k1} - T_{R1}}{T_{b1k2} - T_{R2}} \right)} \quad (5)$$

where T_{R1} and T_{R2} are the inlet and outlet refrigerant temperatures.

Reynolds number. - Reynolds number for the heat exchanger was calculated from

$$\text{Re} = \frac{(\dot{m}_1 / A_m) d}{\mu} \quad (6)$$

where \dot{m}_1 is the mass flow rate from the upstream rake, d is the diameter of the heat exchanger tube (2.54 cm (1 in)), A_m is the minimum free flow area in the heat exchanger, and μ is the viscosity evaluated at the upstream bulk temperature, T_{b1k1} .

Overall heat transfer coefficient. - The product of overall heat transfer coefficient and total heat transfer area was calculated from

$$UA_0 = Q/\text{LMTD} \quad (7)$$

Pressure drop. - The dimensionless pressure drop was calculated from

$$\frac{\Delta P}{q} = \frac{P_{s1} - P_{s2}}{q} \quad (8)$$

P_{s1} and P_{s2} were the average upstream and downstream static pressures respectively, and q was the dynamic pressure upstream of the heat exchanger calculated from

$$q = \frac{1}{2} \left(\frac{\dot{m}_1}{A_f} \right)^2 \frac{RT_{b1k1}}{P_{s1}} \quad (9)$$

A_f is the duct cross-sectional area immediately upstream of the heat exchanger and R is the ideal gas constant for air.

ERROR ANALYSIS

An error analysis was performed using the method of Kline and McClintock (ref. 3). This method requires the estimation of errors in each measured quantity then combines these estimates into an error estimate for the final parameters of interest, i.e., Reynolds number, $\Delta p/q$, etc. Pressure measurement error for the ESP system was estimated as ± 20.7 Pa (± 0.003 psi) based on experience with the system. The type E thermocouples were estimated to have a calibration error of ± 0.25 percent of the difference between the measured

temperature and the reference temperature. Errors in the reference temperature were not considered important. The error in calibration of the strain gauge transducers used for refrigerant pressure measurements was estimated to be ± 345 Pa (± 0.05 psia).

In addition to these instrument errors, there were errors due to the digitization and electronic noise in the ESCORT system (ref. 2).

These errors were estimated for each data channel by calculating the standard deviation of the 20 scans for each channel. The total error estimate for each data channel was then computed as:

$$\text{Total error} = \sqrt{(\text{instrument error})^2 + (\text{std. dev})^2} \quad (10)$$

There is no error analysis that can account for systematic errors in the measurements. In these tests water sprays, frost, and ice continually contaminated the static pressure taps. Engineering judgement was used to eliminate "bad" static tap readings from the data. The total pressure rakes were purged with air when not in use and were not subjected to this problem.

The average errors for all the data points were found to be:

Reynolds number, percent	7.4
Overall heat transfer coefficient, percent	11.8
$\Delta p/q$, percent	4.5

Errors at the low flow rates were much larger (see table III). This was because the total pressures were too small to be measured accurately by the pressure measuring system.

RESULTS AND DISCUSSION

Overall heat transfer and air side pressure drop characteristics of a heat exchanger proposed for use in the NASA Lewis Altitude Wind Tunnel (AWT) have been tested under dry and icing conditions in the Icing Research Tunnel.

Dry Pressure Drop

The ratios of heat exchanger static and total pressure drops to dynamic pressure upstream of the heat exchanger as a function of Reynolds number are shown on figure 8. The asterisk and octagon symbols represent data that were taken before any icing sprays and for less than 6 min accumulation of frost due to condensation of humidity from the air. The square and diamond symbols represent data taken with dry air which allowed longer periods of running with virtually no frost buildup on the coils. This was accomplished by cooling the IRT to 244 K (-20 °F) and running it at a moderate speed for about 1/2 hr. The IRT heat exchanger removed moisture from the air and lowered the dew point to around 242 K (-25 °F). Static pressures, represented by the asterisk and square symbols, were the most difficult quantities to measure accurately due to moisture, ice, and frost buildup on and in the taps. For this reason the total pressure drop was computed by averaging the pressures from the upstream

and downstream rakes and subtracting these two averages. These are the octagon and diamond symbols. Good agreement is obtained between total and static pressure drops. It is not known why there is such a large scatter between the data taken with humid and dry air at the higher Reynolds numbers. The data of figure 98(a), reference 4 most closely matched the AWT heat exchanger parameters. This data was curve fit and converted to the Reynolds number and pressure drop-dynamic head ratio used in this report. The resulting relation,

$$\frac{\Delta P}{q} = 347.8 \text{ Re}^{-0.265} \quad (11)$$

is also shown in figure 8. In the Reynolds number range of interest, the data of figure 98(a), reference 4 predicts a much higher pressure drop than was measured. Also shown on figure 8 is a curve obtained from a proprietary correlation for the pressure drop across a bank of finned tubes. The two correlations predict nearly the same pressure drop.

Dry Heat Transfer

The AWT heat exchanger was designed to have a 4:1 refrigerant overfeed, i.e., refrigerant exits the heat exchanger as three parts liquid and one part vapor. It was not possible to supply enough refrigerant to the test segment to obtain this condition. Refrigerant entered the heat exchanger as a sub-cooled liquid, boiled to a vapor, and exited the heat exchanger with several degrees of superheat. This was thought to be acceptable for the purposes of measuring the dry heat transfer performance and investigating icing behavior.

The multiple refrigerant phases present in the heat exchanger plus the lack of a refrigerant flow rate measurement made it impossible to measure directly a refrigerant side heat transfer coefficient. The only heat transfer measurements possible were the overall heat transfer coefficient. The overall heat transfer coefficient data based on air side area are shown in figure 9. The asterisk symbols are the humid air data and the squares represent the dry air data.

To compare the measured data with existing correlations for air side heat transfer, the refrigerant side heat transfer coefficient must be known. As explained previously, it was not possible to measure this directly. A refrigerant side heat transfer coefficient was estimated from the data by minimizing the least squares function

$$F = \sum_{i=1}^n (U_{\text{meas}} - U_{\text{cal}})^2 \quad (12)$$

where U_{meas} are the n measured overall heat transfer coefficients and U_{cal} the corresponding calculated overall heat transfer coefficients (neglecting tube wall resistance),

$$U_{\text{cal}} = \frac{1}{\frac{1}{h_a n} + \frac{A_o}{h_R A_R}} \quad (13)$$

h_a is the air side heat transfer coefficient calculated using a proprietary correlation for a bank of finned tubes, h_R is the refrigerant side heat transfer coefficient to be determined. A_o and A_R are the air and refrigerant side areas respectively. η is the air side efficiency

$$\eta = [A_o - A_{fin}(1-\eta_{fin})]/A_o \quad (14)$$

where A_{fin} is the total fin area and η_{fin} is the fin efficiency determined by the method in reference 5. The function, F , is minimized by varying h_R . The best estimate for h_R was found to be $1883 \text{ W/m}^2 \text{ }^\circ\text{C}$ ($332 \text{ Btu/hr-ft}^2\text{-}^\circ\text{F}$). This seems to be a reasonable value considering that it must be an average over a tube which contains refrigerant in the liquid, two phase, and vapor states. Also shown on figure 9 is the overall heat transfer coefficient calculated using the proprietary correlation and the data in figure 98(a) of reference 4 to calculate h_a .

A curve fit of the data in figure 98(a) reference 4 gave

$$h_a = 0.032 \frac{k_{air}}{4r_h} \text{Re}^{0.67} \text{Pr}^{1/3} \quad (15)$$

where k_{air} is the thermal conductivity of air evaluated at the mean temperature, r_h is the hydraulic radius, and Pr is the Prandtl number for air. h_R was fixed at $1883 \text{ W/m}^2 \text{ }^\circ\text{C}$ ($332 \text{ Btu/hr-ft}^2\text{-}^\circ\text{F}$). There is good agreement between the calculated and measured overall heat transfer coefficients.

Comparison of Dry Measurements with AWT Requirements

Pressure Drop. - The maximum pressure drop for the AWT heat exchanger will occur at the highest mass flow rate. This will be at the 0.52 Mach number at 1528 m (5014 ft) altitude (table I). At this condition, the Reynolds number for the heat exchanger, based on tube diameter and upstream conditions, is 37 740. From figure 8 the maximum $\Delta p/q$ at this Reynolds number would be about 16. The dynamic pressure, q , would be

$$q = \frac{1}{2} \left(\frac{11806}{3930} \right)^2 \frac{53.35(528)}{2116.3} \frac{27.68}{32.2(144)} = 0.36 \text{ in H}_2\text{O} \quad (16)$$

then

$$\Delta p = 16(0.36) = 5.7 \text{ in H}_2\text{O} \quad (17)$$

This pressure drop is for the heat exchanger only and does not include the additional "blister" losses (i.e., losses due to the extra wide angle diffuser upstream of the heat exchanger, see figure 1.).

Heat transfer. - Maximum required heat exchanger overall heat transfer coefficient - area product, UA is $1.445 \times 10^6 \text{ W/}^\circ\text{C}$ ($2.7406 \times 10^6 \text{ Btu/hr-}^\circ\text{F}$) and occurs at the 0.7 Mach number 33 215 ft altitude condition (table I). The Reynolds number at this condition based on tube diameter and conditions upstream of the heat exchanger is 19 615. From the lower curve on figure 9,

the overall heat transfer coefficient at this Reynolds number is 1.308 W/m²°C (7.43 Btu/hr-ft-°F). To scale to AWT heat exchanger area the air side area of the segment tested in IRT will be multiplied by the ratio of face areas i.e.,

$$(UA)_{AWT} = (UA)_{SEG} \frac{(A_f)_{AWT}}{(A_f)_{SEG}} = (7.43)(1046.15) \frac{3930(144)}{36(35.4)} \quad (18)$$

This relation gave a (UA)_{AWT} of 1.82x10⁶ W/°C (3.45x10⁶ Btu/hr-°F) which is 26 percent larger than the required UA.

Frost Buildup

The effect of running humid air over the cold heat exchanger coils was investigated. The heat exchanger coils were kept at 241 K (-25 °F) and air flow was maintained at the maximum speed. The dew point of air was measured to be 273 K (32 °F). After approximately 30 min of running the coils were nearly blocked with frost buildup. This buildup was virtually uniform from front to back of the heat exchanger. The cold coils of the heat exchanger make a very efficient dehumidifier; it is therefore recommended that AWT be started with dry air, to minimize loss of performance due to frost buildup.

Icing

Heat transfer and pressure drop data for the AWT heat exchanger segment were taken for several icing conditions. Three test section total temperatures, 244, 255, and 264 K (-20, 0, and +15 °F) (nominal temperatures measured upstream of the IRT test section) were run as well as two drop sizes, 15 and 30 μm. All icing tests were conducted at a 1.36 gm/m³ LWC in the IRT test section. To achieve the same LWC at the actual AWT heat exchanger a higher LWC in the AWT test section would be required due to the difference in the heat exchanger-test section area ratios between the IRT and AWT as well as the anticipated difference in the fraction of cloud removed upstream of the heat exchanger between the IRT and AWT. The values of AWT test section LWC that would produce the same LWC at the heat exchanger as those tested would be 1.49 gm/m³ for the 15 μm drops and 1.71 gm/m³ for the 30 μm drops. These values were estimated using the relationship

$$(LWC)_{AWT} = (LWC)_{IRT} \frac{(A_{hx}/A_{TS})_{AWT}}{(A_{hx}/A_{TS})_{IRT}} \frac{(1-X_{IRT})}{(1-X_{AWT})} \quad (19)$$

where (LWC)_{IRT} is the liquid water content in the IRT test section, (A_{hx}/A_{TS})_{AWT} and (A_{hx}/A_{TS})_{IRT} are the area ratios between the heat exchanger and test section cross sections for the AWT and IRT respectively (12.51 and 13.96 respectively). X_{IRT} and X_{AWT} are the fraction of the icing cloud removed by the turning vanes, screens and fan for the IRT and AWT respectively. These were estimated from figure 10(a),(b), which were taken from reference 6. These two test points are shown by the symbols on figure 2. Tests were also conducted with and without refrigerant flowing through the heat exchanger to determine the effect of surface temperature on ice growth rate.

Ice buildup. - For all conditions tested, ice buildup on the heat exchanger coils had the same characteristics. Ice formed only on the leading edges of the fins and tubes that were in direct line-of-sight from upstream. Ice formed on the second row of tubes only on the fin leading edges directly downstream of the gap between tubes in the first row. The ice accretion can be seen in figure 11. Some of the ice was knocked off before the photograph was taken to give a better idea of the quantity of ice accreted. This photo was taken after 50 min spray at 264 K (+15 °F) with 15 μm drops at an AWT test section equivalent 1.49 gm/m^3 LWC.

Effect of air temperature. - Total and static pressure drop - dynamic pressure ratios are plotted versus ice accretion time for 244, 255, 264 K (-20, 0, and +15 °F) test conditions in figure 12. For all these data the IRT was run at a constant test section speed of 67 m/s (150 mph), the drop size was 15 μm and the liquid water content was 1.36 gm/m^3 in the IRT test section (AWT equivalent LWC is 1.49 gm/m^3). Although there is some scatter in the 0 and 15 °F data the trend is clearly toward faster ice buildup at colder temperatures. At the 244 K (-20 °F) temperature the pressure drop-dynamic head ratio increases by a factor of 2.3 in 15 min of icing. During icing tests the fan in the AWT heat exchanger duct was run full speed with the fan damper wide open. As ice built up the flow rate and thus Reynolds number decreased as shown on figure 13.

Effect of drop size. - Figure 14 shows the pressure drop-dynamic head ratio for drop sizes of 15 and 30 μm . It is clear that smaller drop sizes cause the heat exchanger to plug with ice in a shorter time. As seen from figure 10(a), the larger the drop size the more water is removed before reaching the heat exchanger; thus, the LWC at the heat exchanger will be lower for larger size drops. This is opposite to the trend shown in figure 14. During the heat exchanger tests, LWC was measured at the heat exchanger location. This involved measuring the drop size using the soot slide technique. With this technique a slide that was coated with lamp black (soot) was exposed for a brief time to the air stream containing the water drops. The drops impinge on the slide and cause a "crater" in the soot. The diameter of these craters can be correlated to drop size. With the 30 μm drops the craters were round indicating spherical liquid water drops were still present. With the 15 μm drops many of the craters were jagged as if ice crystals had struck the soot instead of liquid water. The presence of all ready frozen ice crystals could be the cause of the formation of less dense ice and thus faster buildup with smaller drop sizes.

Effect of surface temperature. - The effect of heat exchanger surface temperature is shown on figure 15. Two temperatures were obtained by flowing or not flowing refrigerant through the heat exchanger. For the no refrigerant case the surface temperature was determined by the air temperature and was measured to be about 0.6 °C (1 °F) higher than the air temperature. With refrigerant flowing the difference between air temperature at the inlet to the heat exchanger and the first row coil surface temperature was about 6.7 °C (12 °F). A discontinuity is apparent in the data with refrigerant off. It is believed that the data after 10 min of icing spray with the refrigerant off is in error and that there is no effect of heat exchanger surface temperature (unless of course the air is above freezing). This is substantiated by visual observation of the ice buildup; no difference could be seen between the two cases for the same ice accretion times.

Heat transfer. - The effect of ice accretion on overall heat transfer coefficient is shown on figure 16. This test was conducted at 244 K (-20 °F), 15 μm drops and an equivalent AWT test section liquid water content of 1.49 gm/m³. The initial Reynolds number for this test was 57 800. This corresponds to full flow for the heat exchanger duct. As ice built up on the coils the flow rate and thus Reynolds number decreased (fig. 13). The heat transfer coefficient is seen to rise slightly for about the first 6 min of icing. This is probably due to the increased roughness caused by ice accretion. The heat transfer then falls off as the flow is reduced due to the higher pressure drop. Figure 16 shows that the overall heat transfer coefficient is much less sensitive than the pressure drop to ice accumulation.

CONCLUSIONS

Air side pressure drop and overall heat transfer characteristics of a heat exchanger proposed for use in the NASA Lewis Altitude Wind Tunnel have been tested in the Icing Research Tunnel under dry and icing conditions. The objective of these tests was to determine if the proposed heat exchanger could meet the requirements of AWT. The conclusions are:

1. The proposed heat exchanger exceeds the design heat transfer requirements by 26 percent.
2. Dry pressure drop is reasonable at 1420 Pa (5.7 in of water) (heat exchanger only - not including wide angle diffuser ("blister") losses).
3. Frost forms uniformly on all heat exchanger surfaces, consequently AWT cannot be started with moist air.
4. Ice forms only on fin and tube leading edges that are in direct line-of-sight to oncoming stream.
5. Ice builds up faster at the colder air temperatures - dimensionless pressure drop doubles after 10 min icing with 15 μm drops at 244 K (-20 °F); completely blocked in 20 to 30 min at this condition.
6. Ice builds up faster with smaller drop sizes probably due to freezing of water drops into ice crystals before contact with heat exchanger surface.
7. Surface temperature has little or no effect on ice accretion rate if air temperature sufficiently below freezing.

REFERENCES

1. Anon., "Altitude Wind Tunnel For Propulsion and Icing Research," Preliminary Engineering Report, Section 9, Process Systems 50 percent review, April 20, 1984 prepared by Sverdrup Corp. St. Louis, MO. for NASA Lewis contract number NAS3-24024-AE.
2. Miller, R.L., "ESCORT: A Data Acquisition and Display System to Support Research Testing," NASA TM-78909, 1978.

3. Kline, S.J., and McClintock, F.A., "Describing Uncertainties in Single-Sample Experiments," Mechanical Engineering, Vol. 75, Jan. 1953, pp. 3-8.
4. Kays, W.M., London, A.L., Compact Heat Exchangers, National Press, Palo Alto, CA., 1955, p. 116.
5. Schneider, P.J., Conduction Heat Transfer, Addison-Wesley Publishing Co, Inc., 1955, pp. 83-84.
6. Newton, J., "An Ice Accretion Study on an Icing Research Tunnel," to be presented at AIAA 1986 Aerospace Sciences Meeting, Reno, Nevada. NASA TM-87095.

TABLE I. - HEAT EXCHANGER SEGMENT PARAMETERS

Minimum free flow area, A_m	0.419 m ² (4.506 ft ²)
Total air side heat transfer area, A_o	97.2 m ² (1046.15 ft ²)
Free flow area/frontal area, A_m/A_f	0.509
Total fin area, A_{fin}	91.22 m ² (981.9 ft ²)
Fin area/total area, A_{fin}/A_o	0.939
Refrigerant side heat transfer area, A_R	6.08 m ² (65.46 ft ²)
Surface area/volume	340.9 m ² /m ³ (103.9 ft ² /ft ³)
Hydraulic diameter, $4r_h$	0.549 cm (0.018 ft)

TABLE II. - REQUIRED HEAT EXCHANGER PERFORMANCE AT VARIOUS CONDITIONS
(-55 °F FLOODED COIL)

[Total Heat Load = $Q_{fan} + Q_{ice} + Q_{steam}/heat$.]

Number	Mach number	Altitude, ft	Temperature, °F	Heat load $\times 10^{-6}$, Btu/hr	Mass flow, lbm/sec	LMTD, °F	Re	$UA \times 10^{-6}$, Btu/hr-°F
1	0.20	762	439.7	128.77	5 484	46.9	19 608	2.7406
2	.20	23 163	439.7	23.47	2 353.7	40.1	8 645	0.5839
3	.30	1 710	521.8	32.26	7 607.6	119.	24 780	.2705
4	.30	24 366	439.7	39.6	3 368.7	41.1	12 328	.9628
5	.40	3 012	524.5	68.29	9 713.5	123.	31 368	.5528
6	.40	26 012	439.7	60.66	4 208.6	42.4	15 320	1.4274
7	.52	5 014	527.9	120.08	11 806	128.	37 740	.9330
8	.52	28 522	439.7	88.19	4 948.1	44.2	17 890	1.9945
9	.60	14 875	499.2	114.89	9 639	100.	32 045	1.1381
10	.60	30 483	439.7	107.7	5 268.9	45.5	18 956	2.3665
11	.70	25 000	471.7	163.66	7 665.9	78.4	26 140	2.0873
12	.70	33 215	439.7	128.77	4 584	46.9	19 615	2.7406
13	.80	32 000	456.6	167.93	6 595.5	65.2	22 862	2.5744
14	.80	55 000	439.9	102.28	2 239.3	57.3	7 680	1.7841
15	.84	34 000	453.3	169.26	6 340.5	62.4	22 040	2.7085
16	.84	55 000	444.6	108.64	2 341.9	62.6	7 963	1.7338
17	.92	55 000	455.4	119.98	2 564.2	74.2	8 569	1.6160

$m = 0.3048 \times ft$.

Watt = $0.2929 \times Btu/hr$.

kg/sec = $0.4536 \times lbm/sec$.

deg K = $(°F + 459.67) 1.8$.

W/°C = $0.5275 \times Btu/hr-°F$.

TABLE III. - HEAT TRANSFER AND PRESSURE DROP DATA

Rdg. number	Re	Error, %	U_1 Btu/hr-ft ² -°F	Error, %	$\frac{\Delta P_s}{q}$	Error, %	LMTD, °F	Error, %	t_{ice} , min	t_{frost} , min	Drop size, μ m
25.	46830.8	2.4	8.78	4.0	12.64	0.4	42.17	1.4	0.0	11.0	0.0
26.	46396.7	2.4	7.34	7.6	13.19		42.37	2.0		16.0	
27.	46446.7	2.4	8.78	3.4	13.36		40.22	1.6		21.0	
28.	45065.9	2.5	8.89	3.1	14.48		39.25	1.7		26.0	
29.	44902.8	2.5	9.62	3.4	14.73		38.38	1.8		31.0	
30.	26764.1	7.6	7.20	7.9	14.89	1.3	38.83	1.5		6.0	
31.	28858.8	6.1	7.90	6.6	14.16	0.9	38.60	1.9		11.0	
32.	28473.2	6.3	8.02	6.8	15.77	0.9	37.86	2.1		16.0	
33.	27746.7	6.7	8.02	7.5	17.91	0.8	37.19	2.5		22.0	
34.	27492.3	6.7	7.95	7.4	19.30	0.8	36.93	2.5		27.0	
35.	26190.6	7.4	7.87	8.2	22.46	0.7	36.00	2.6		32.0	
36.	25911.9	7.6	7.81	8.7	24.07	0.7	35.59	2.9		41.0	
38.	23217.6	9.4	7.39	10.9	12.79	1.6	37.20	2.8		7.0	
39.	18387.9	16.6	5.95	17.5	24.27	1.3	36.98	3.0		12.0	
40.	18467.2	17.0	6.05	18.0	27.02	1.2	36.48	3.2		17.0	
41.	17936.9	17.7	5.93	19.3	31.47	1.1	36.19	4.0		22.0	
42.	13411.6	47.9	4.80	48.2	61.53	1.0	35.27	3.4		27.0	
43.	12161.6	33.9	4.40	34.5	80.15	0.9	34.91	3.8		32.0	
44.	11373.5	39.5	4.22	40.0	97.64	0.9	34.69	4.0		37.0	
45.	14512.9	26.4	5.15	27.8	63.26	0.8	35.42	4.9		42.0	
47.	41331.0	3.4	6.65	4.1	18.95	0.4	41.79	1.4		5.0	
48.	37648.5	3.9	6.55	4.4	26.16	0.4	43.21	1.4		10.0	
49.	33508.6	4.5	6.44	6.0	37.12	0.3	43.70	1.6		15.0	
50.	27211.9	6.7	5.76	10.5	58.81	0.6	43.87	2.6		20.0	
51.	18555.9	15.8	4.72	16.5	125.63	0.3	43.09	1.9		25.0	
52.	10843.6	45.0	3.49	45.3	377.61	0.3	41.91	1.9		30.0	
54.	62055.3	2.0	11.23	7.5	10.66	0.4	7.36	6.1		0.0	
55.	59257.7	2.1	11.09	7.7	12.92	0.3	7.28	6.4	5.0		15.0
56.	57421.9	2.2	11.42	8.3	15.17	0.3	6.45	6.9	10.0		15.0
57.	44716.8	3.7	11.56	9.4	34.07	0.3	5.86	7.9	20.0		15.0
58.	14054.7	42.5	5.80	44.2	345.78	0.2	5.50	9.0	30.0		15.0
60.	55720.9	2.2	9.40	17.0	10.18	0.5	5.13	7.6	0.0		0.0
61.	49917.5	2.4	7.28	12.8	14.55	0.4	4.35	7.5	5.0		15.0
62.	49804.2	2.5	7.83	10.2	15.48	0.4	4.49	7.4	10.0		
63.	45753.4	2.9	8.16	10.5	19.21	0.3	4.23	7.9	15.0		
64.	50482.0	2.4	8.90	12.4	15.06	0.3	3.46	9.5	20.0		
65.	49132.3	2.5	9.24	11.6	16.44	0.3	3.65	9.1	25.0		
66.	45104.4	2.9	9.15	11.9	21.64	0.3	3.56	9.6	35.0		
67.	33940.3	5.1	6.77	14.1	42.98	0.3	3.22	10.8	50.0		
70.	57796.3	2.1	10.91	8.0	11.73	0.4	7.03	6.6	0.0		0.0
71.	58356.2	2.6	11.29	8.7	11.86	0.4	6.51	7.1	2.0		15.0
72.	58516.9	2.1	11.81	8.6	12.81	0.4	6.65	7.3	5.0		
73.	53722.9	2.5	11.47	8.7	16.95	0.3	6.60	7.4	10.0		
74.	45618.6	3.4	10.64	8.8	26.88	0.3	6.67	7.3	15.0		
75.	24321.9	12.8	7.80	15.5	105.20	0.3	5.97	8.0	20.0		
77.	51376.8	2.1	10.95	8.1	10.74	0.5	7.33	5.0	0.0	6.0	0.0
78.	56034.0	2.1	9.56	7.8	11.21	0.4	6.82	6.1	0.0	0.0	15.0
79.	53951.4	2.3	9.21	9.5	13.04	0.4	5.38	7.1	5.0		
80.	52041.0	2.4	9.54	12.6	14.95	0.3	4.77	8.3	10.0		
81.	49378.7	4.8	9.40	10.3	17.46	0.4	5.28	7.7	15.0		
82.	51334.1	2.5	10.01	9.4	16.83	0.3	5.19	7.6	20.0		
83.	30504.2	7.0	7.82	14.4	60.04	0.6	4.38	10.6	30.0		
93.	58491.0	2.2	11.31	8.7	11.80	0.4	6.40	7.1	0.0		0.0
94.	57782.4	2.2	10.72	9.0	12.71	0.4	6.28	7.2	5.0		30.0
95.	58067.2	2.2	11.05	9.1	13.14	0.3	5.90	7.5	10.0		
96.	57032.0	2.4	11.39	10.2	14.52	0.4	5.78	8.1	15.0		
97.	55285.0	2.4	11.23	9.8	15.96	0.3	5.76	7.9	20.0		
98.	54270.7	2.6	11.53	10.0	17.07	0.5	5.32	8.4	25.0		
99.	49907.1	2.8	11.51	10.0	22.60	0.3	5.43	8.6	35.0		
100.	39607.4	4.7	11.39	11.5	42.74	0.3	5.08	9.8	45.0		
111.	39369.7	5.0	9.36	8.2	13.36	0.8	9.09	5.8	0.0		0.0
112.	29691.4	10.0	8.58	12.2	15.11	1.3	8.87	6.1			
113.	42184.3	4.3	9.46	8.0	16.04	0.6	8.78	5.9			
114.	50626.1	3.0	10.27	7.6	15.28	0.4	8.84	5.9			
115.	55273.3	2.6	10.59	7.5	15.02	0.4	8.66	5.9			
116.	58635.9	2.4	11.03	7.6	15.24	0.4	8.55	6.2			
117.	32657.1	7.4	9.46	10.3	13.31	1.3	8.38	6.3			
118.	49622.6	3.2	10.59	7.8	14.75	0.5	8.49	6.2			
119.	60176.5	2.2	11.12	7.6	15.09	0.4	8.41	6.1			

$W/m^2 \text{ } ^\circ C = 0.1761 \times \text{Btu/hr-ft}^2\text{-}^\circ F.$

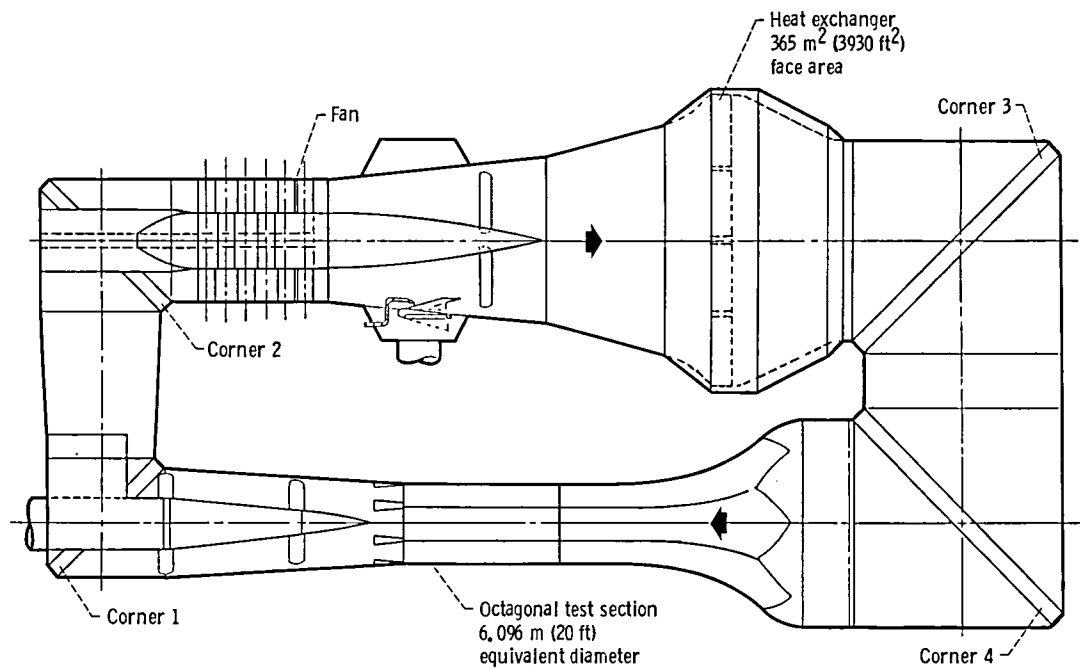


Figure 1. - Schematic of the altitude wind tunnel with proposed modifications.

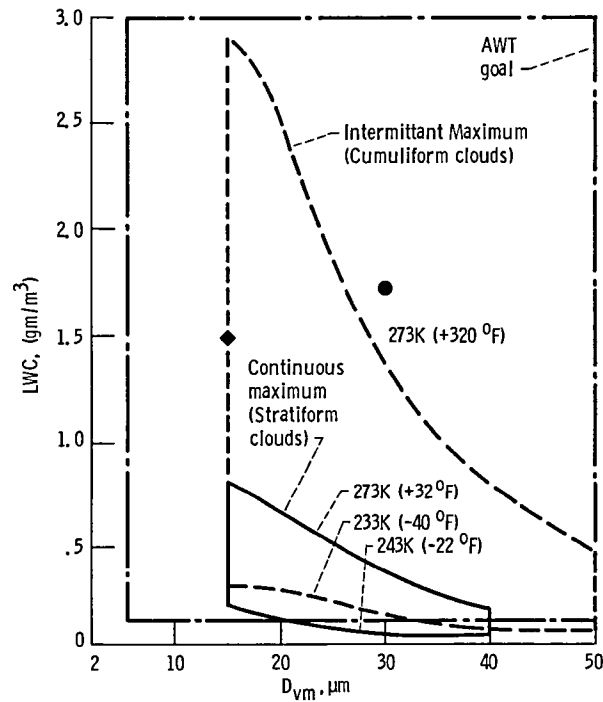


Figure 2 - AWT icing goal and FAR 25 icing envelope.

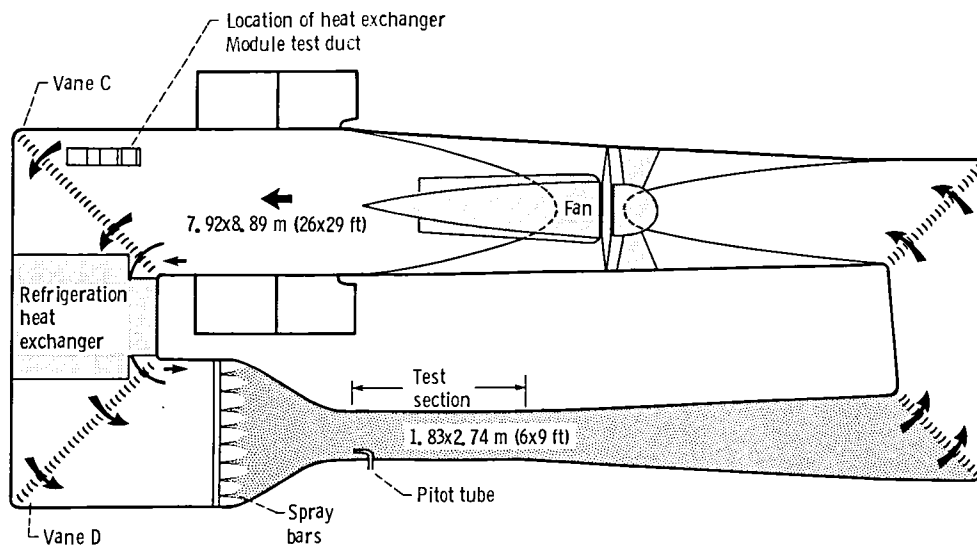


Figure 3. - Schematic of icing research tunnel.

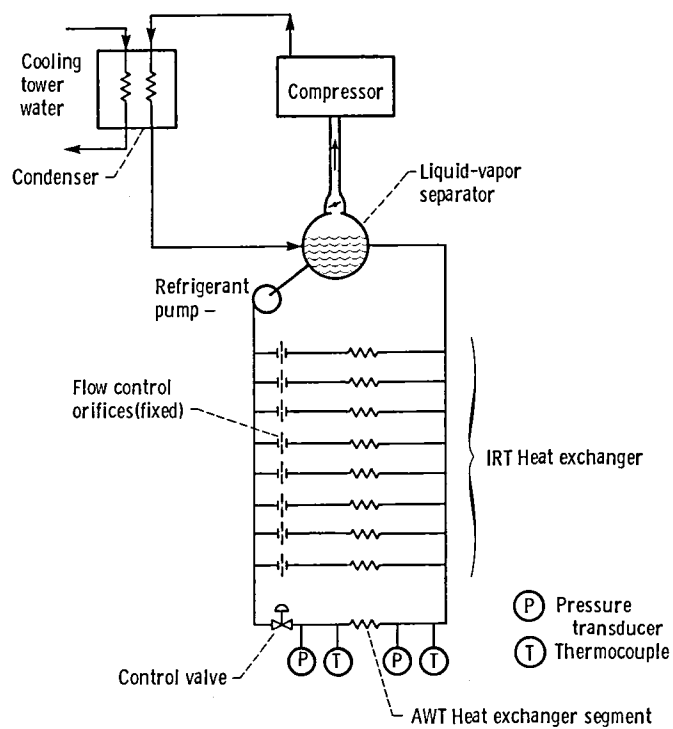
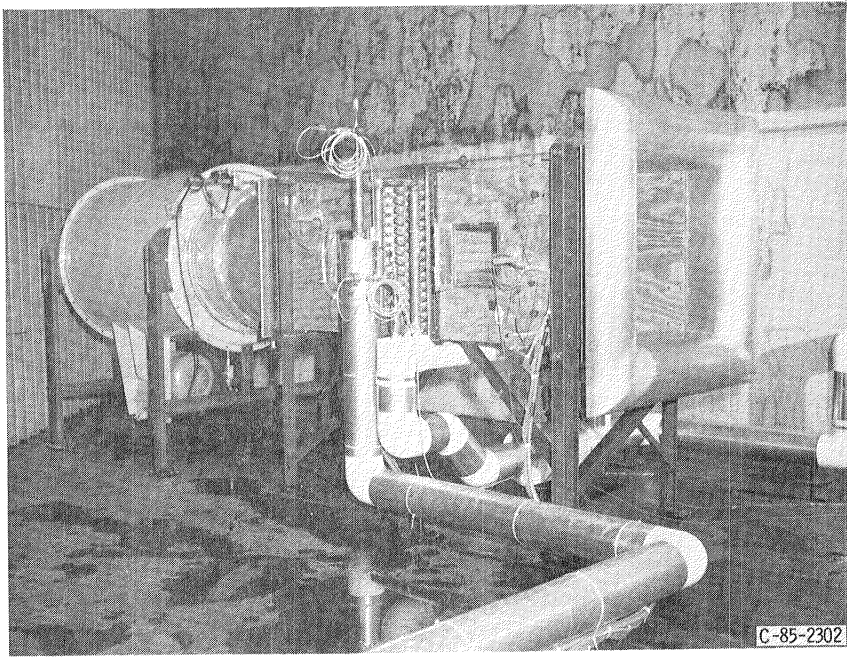
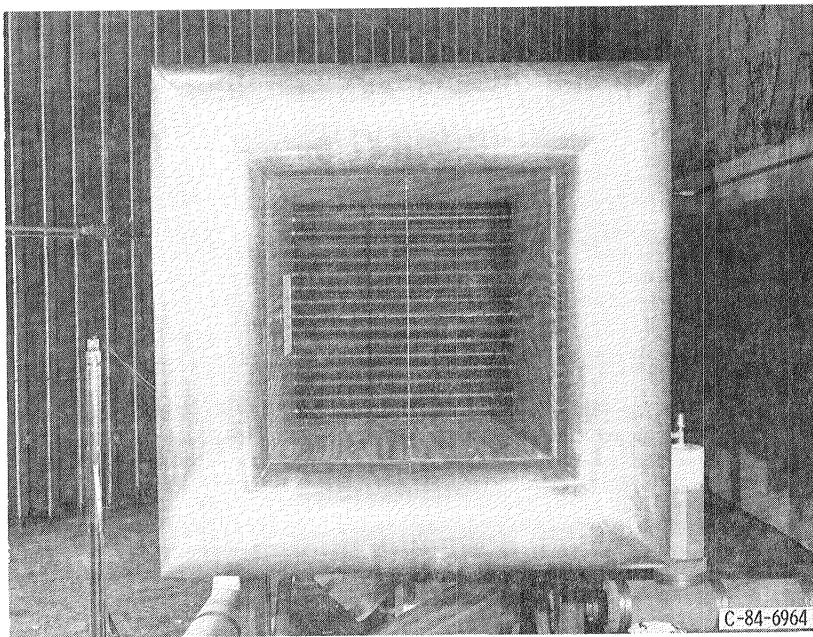


Figure 4. - IRT refrigeration system with AWT heat exchanger segment.



(a) AWT heat exchanger test duct.

Figure 5.



(b) Duct inlet, heat exchanger and upstream rake.

Figure 5.

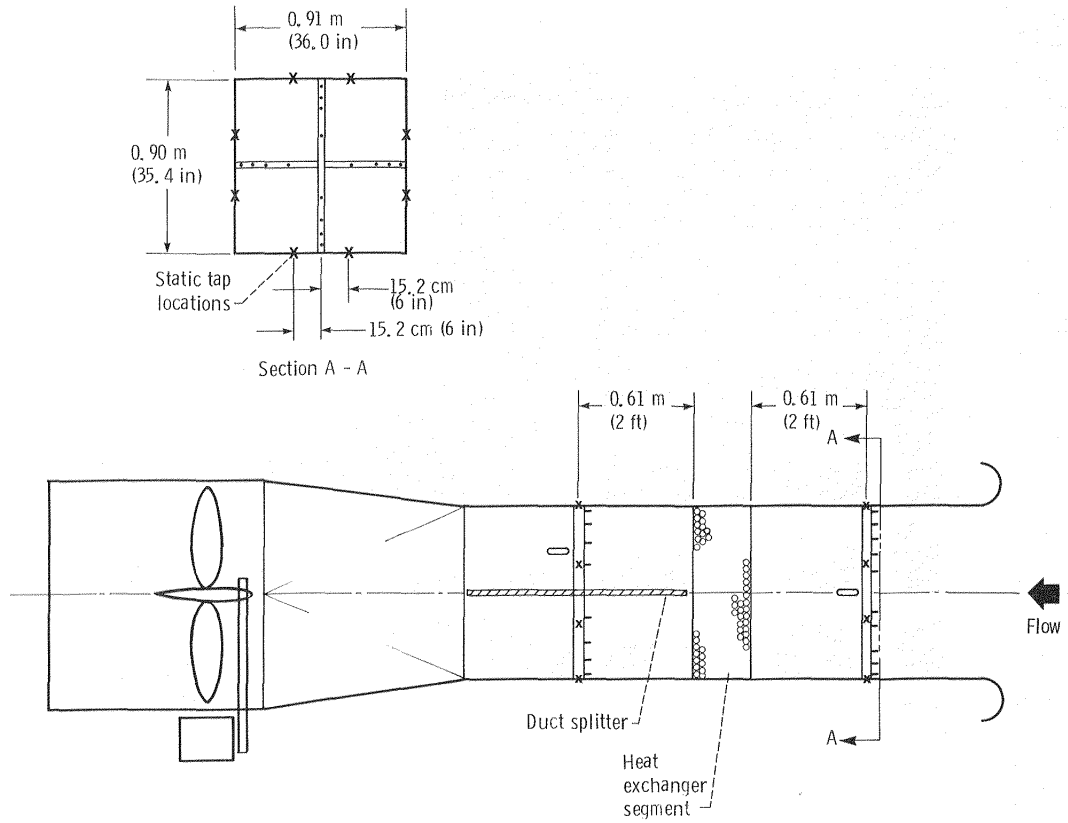


Figure 6. - Schematic of heat exchanger test duct.

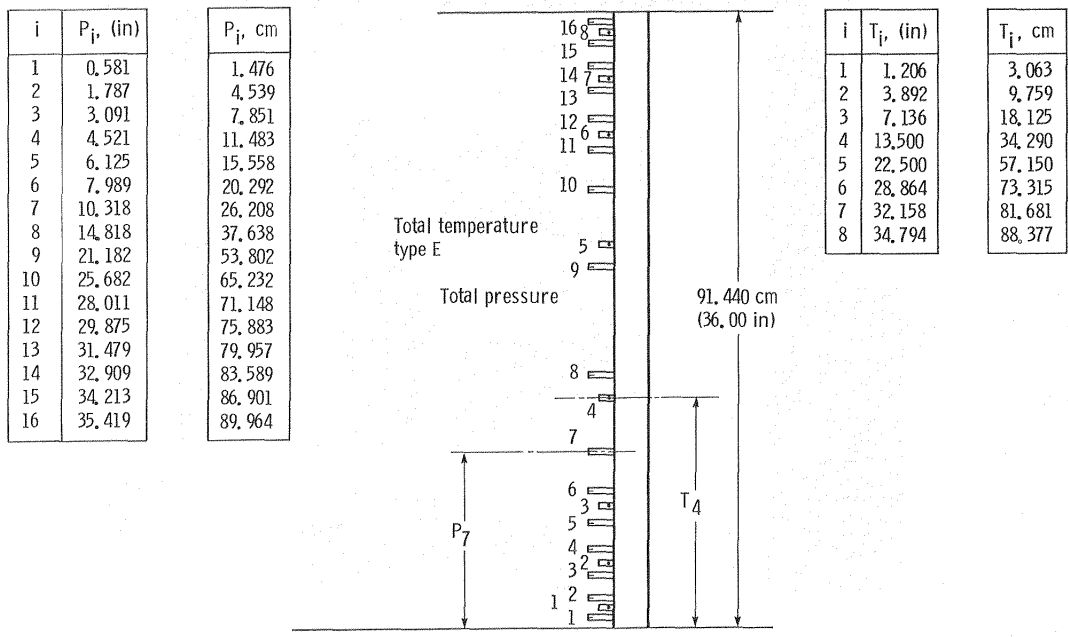


Figure 7. - Temperature-pressure rake for AWT heat exchanger test.

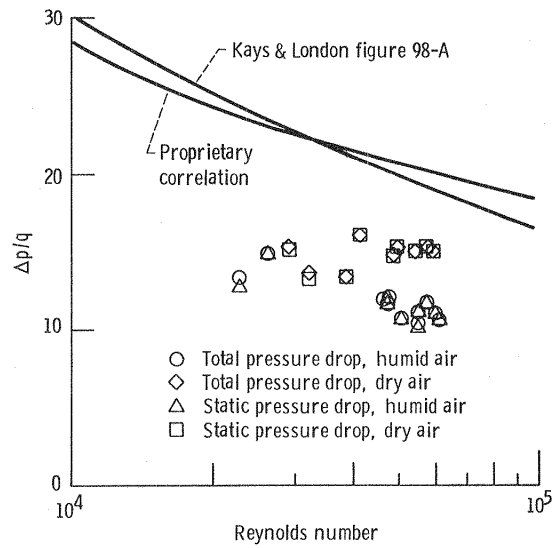


Figure 8. - Total and static pressure drop-dynamic head ratio.

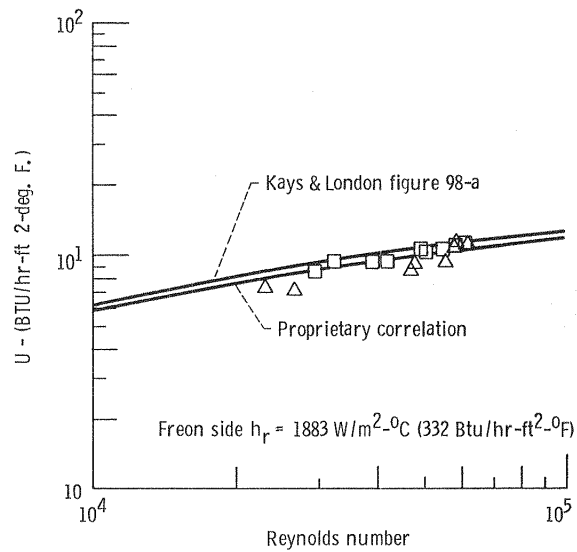
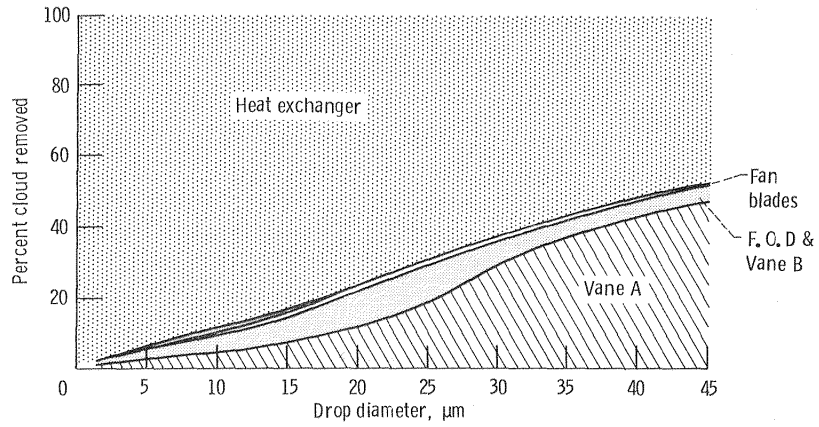
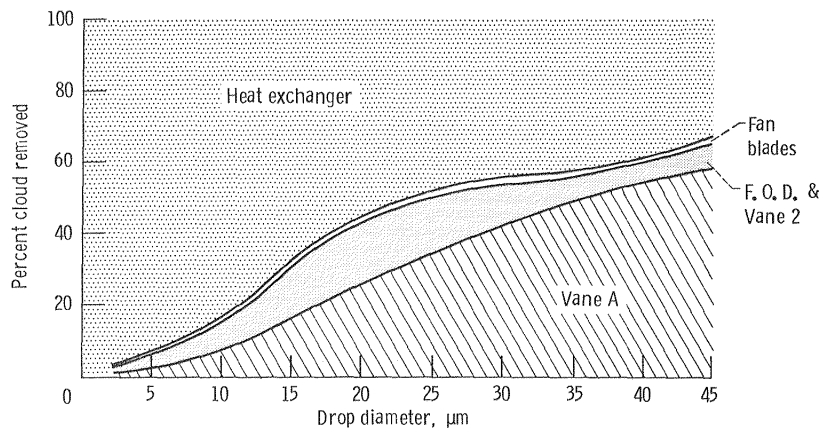


Figure 9. - Heat exchanger overall heat transfer coefficient based on air side area.



(a) Mass balance in the icing research tunnel.

Figure 10.



(b) Mass balance scaled to AWT for worst icing case.

Figure 10. - Concluded.

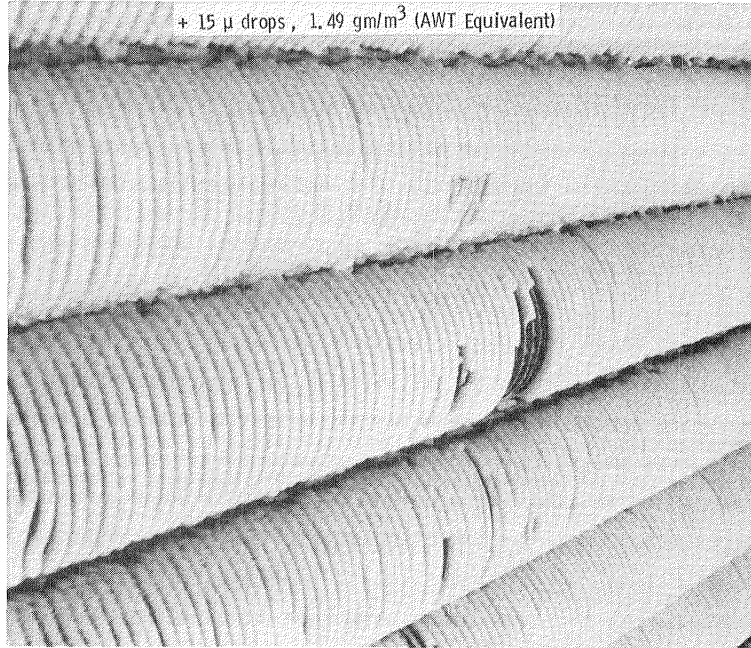


Figure 11. - Ice accretion on front of heat exchanger after 50 minutes of icing spray.

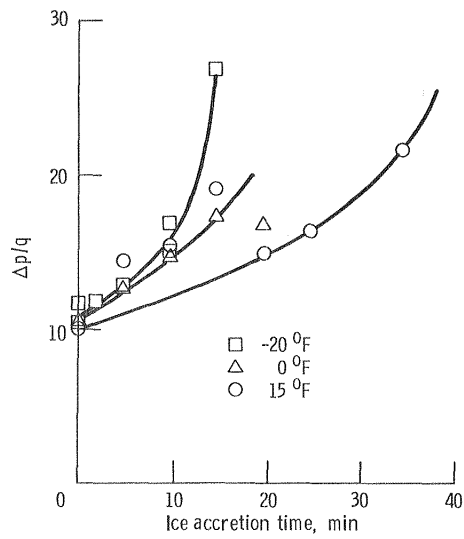


Figure 12. - Effect of temperature on heat exchanger pressure drop due to ice accretion, $15\ \mu\text{m}$ drops, $1.49\ \text{gm}/\text{m}^3$ LWC (AWT equivalent).

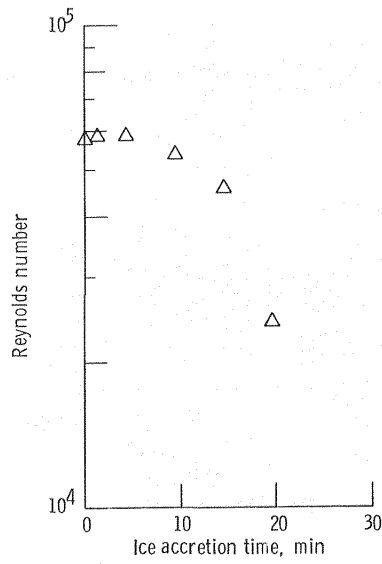


Figure 13. - Effect of ice buildup on Reynolds number for 244 K (-20 °F), 15 μm drops, 1.49 gm/m³ LWC (AWT equivalent).

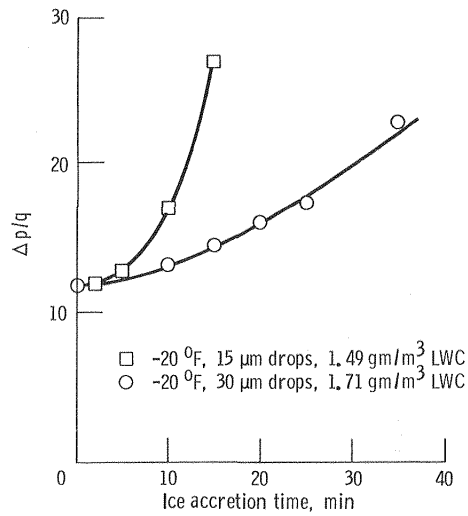


Figure 14. - The effect of drop size on ice accretion rate.

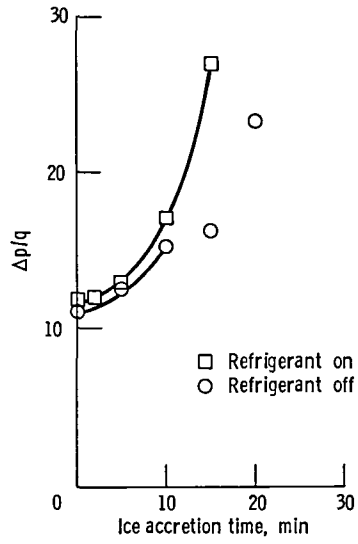


Figure 15. - Effect of heat exchanger surface temperature on pressure drop due to ice accretion for 244 K (-20 °F), 15 μm drops, 1.49 gm/m³ LWC (AWT equivalent).

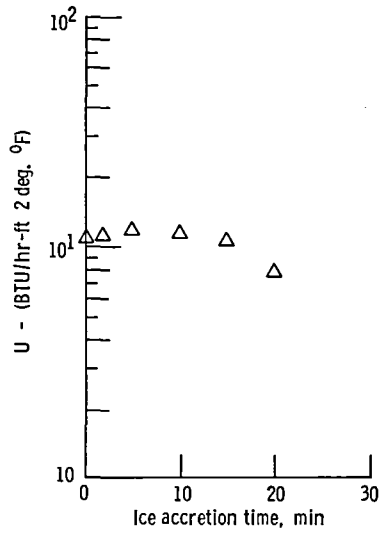


Figure 16. - Effect of ice accretion on heat exchanger overall heat transfer coefficient for 294 K (-20 °F), 15 μm drops and 1.49 gm/m³ LWC (AWT equivalent).

1. Report No. NASA TM-87151		2. Government Accession No.		3. Recipient's Catalog No.	
4. Title and Subtitle Heat Transfer and Pressure Drop Performance of a Finned-Tube Heat Exchanger Proposed for Use in the NASA Lewis Altitude Wind Tunnel				5. Report Date November 1985	
				6. Performing Organization Code 505-40-7A	
7. Author(s) G. James Van Fossen				8. Performing Organization Report No. E-2623	
				10. Work Unit No.	
9. Performing Organization Name and Address National Aeronautics and Space Administration Lewis Research Center Cleveland, Ohio 44135				11. Contract or Grant No.	
				13. Type of Report and Period Covered Technical Memorandum	
12. Sponsoring Agency Name and Address National Aeronautics and Space Administration Washington, D.C. 20546				14. Sponsoring Agency Code	
15. Supplementary Notes					
16. Abstract A segment of the heat exchanger proposed for use the in the NASA Lewis Altitude Wind Tunnel (AWT) facility has been tested under dry and icing conditions. The heat exchanger has the largest pressure drop of any component in the AWT loop. It is therefore critical that its performance be known at all conditions before the final design of the AWT is complete. The heat exchanger segment was tested in the NASA Lewis Icing Research Tunnel (IRT) in order to provide an icing cloud environment similar to what will be encountered in the AWT. Dry heat transfer and pressure drop data were obtained and compared to correlations available in the literature. The effects of icing sprays on heat transfer and pressure drop were also investigated.					
17. Key Words (Suggested by Author(s)) Heat transfer; Icing			18. Distribution Statement Unclassified - unlimited STAR Category 34		
19. Security Classif. (of this report) Unclassified		20. Security Classif. (of this page) Unclassified		21. No. of pages	22. Price*

End of Document